Available online at www.sciencedirect.com
ScienceDirect
Journal of the European Ceramic Society 30 (2010) 3297–3302
www.elsevier.com/locate/jeurceramsoc

Crack mouth opening displacement controlled fracture tests of brittle ceramics

A. García-Prieto, C. Baudín *

Instituto de Cerámica y Vidrio, CSIC, CSIC-Campus de Cantoblanco, Kelsen 5, 28049 Madrid, Spain

Received 23 June 2010; received in revised form 27 July 2010; accepted 2 August 2010

Abstract

Controlled fracture tests are required for the accurate determination of the toughness parameters of materials in order to assure the full conversion of the supplied energy into crack surface energy. From the three parameters involved in the test, load, displacement of the load point and crack mouth opening displacement (CMOD), this latter is the only one that continuously increases as fracture proceeds. Therefore, the CMOD has been proposed as control variable for the stable fracture tests. In this work, a new equipment to perform stable fracture tests of single edge V-notch beams (SEVNB) of ceramics in three points bending controlled by the CMOD is presented. The developed equipment allows performing stable fracture tests of extremely brittle materials. The equipment is presented together with results obtained for fine grained aluminium–magnesium aluminate and alumina ceramics.

Keywords: Al_2O_3; Spinel; Toughness; Stable fracture; Work of fracture

1. Introduction

It is well known that stable crack growth is necessary to get reliable and accurate fracture toughness data. When the fracture toughness values are determined from test configurations that do not allow stable crack growth the calculated toughness value might be over-evaluated (e.g. for a dense α-SiC, $K_{IC} \sim 4$ and 3 MPa $m^{1/2}$ for unstable and stable tests, respectively).[1] Moreover, controlled fracture tests supply much more information about the fracture process than the fast fracture ones because, in addition to the conventional fracture toughness for crack initiation, controlled fracture allows the determination of fracture energy and crack-growth resistance curves.

Fracture toughness tests of ceramics are usually performed in universal testing machines by subjecting the specimens located between the loading supports to increasing deformation by means of the displacement of the loading frame. The deformation of the specimen can be controlled by imposing a constant rate to the increase of the displacement of the frame and, thus, to the loading point (displacement control), the load (load control), the deflection of the specimen directly measured at the central point, in bending specimens, (deflection control) or the crack mouth opening displacement (CMOD control). The simplest and therefore most widely used testing conditions are the control of the specimen deformation by constant rates of increasing displacement or load.

Controlled fracture tests for brittle materials, as most ceramics, are difficult to accomplish, therefore, they are not usually performed. Since the initial works of Nakayama et al.[2,3] and Tattersall and Tappin[4] different authors have developed innovative specimen designs and tests geometries (e.g. 5–10) to attain stable fracture of materials using displacement controlled loading. Such approach has made it possible to reach stable fracture for materials as brittle as glass[2,11] and fine grained MgO[4] using hard machines. In general, the specimens required for these tests are difficult to fabricate especially for brittle ceramics.

From the broad spectrum of available fracture tests, bending of parallelepiped specimens with straight trough notches (SENB) is a relatively simple way of testing and displacement or load controlled bending tests have been widely used for fracture toughness testing of ceramics. Therefore, different attempts to perform stable tests using three point bending loaded beams, which are generally more stable than the four point bending ones,[12] have been done.

* Corresponding author.
E-mail address: cbaudin@icv.csic.es (C. Baudín).

0955-2219/$ – see front matter © 2010 Elsevier Ltd. All rights reserved.
doi:10.1016/j.jeurceramsoc.2010.08.007

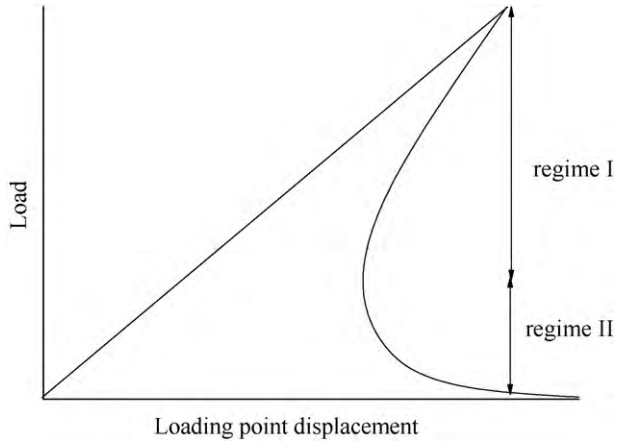

Fig. 1. General load–loading point displacement plot for beams of brittle materials with straight through notches (SENB). The curved part corresponds to the fracture taking place with constant energy release rate, G, equalling G_c. As the straight line that represents the loading of the specimen hits the curve, the condition for crack growth ($G = G_c$) is satisfied. To keep $G = G_c$ the load point displacement has to decrease initially (regime I) and then increase (regime II).

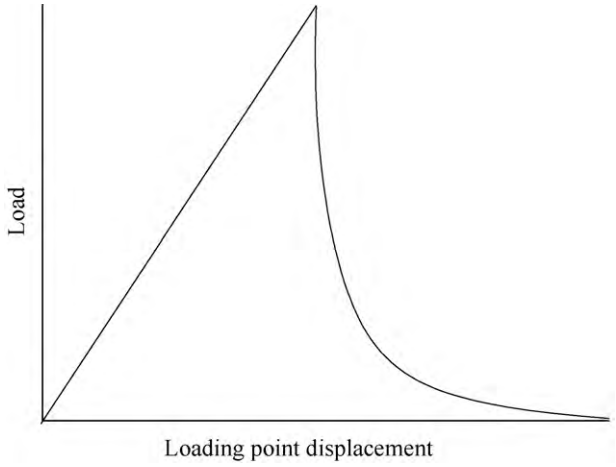

Fig. 2. Load–loading point displacement plot for stable fracture reached using constant displacement rate.

The schematic representation of Fig. 1 allows discussing some aspects about the stable crack growth in SENB specimens of brittle materials, as done by Sigl.[13] The curved line is the general stable fracture locus of a material with flat R curve (Griffith locus, critical energy release rate, G_c = constant). This curve represents the fracture taking place with constant energy release rate, G, equalling G_c. As the straight line that represents the loading of the specimen hits the curve, the condition for crack growth ($G = G_c$) is satisfied. In order to get stable fracture, G has to be maintained at its critical value and, thus, decreasing values of the load point displacement (regime I) followed by increasing values of this parameter (regime II) would be demanded. The load–displacement relationship of regime I is usually called snap back.[14] Therefore, it will not be possible to get stable fracture using constant displacement rates. The relative weight of the regions corresponding to regimes I and II depend on the material properties, the specimen and span sizes, the notch depth and the stiffness of the testing device. For the same material and testing geometry, stiff machines and deep notches increase the region of regime II and situations such as that plotted in Fig. 2 can occur. In this case, stable fracture can be reached controlling by constant displacement rate because increases in displacement after the maximum load still allow to follow the stable condition for crack growth $G = G_c$. In terms of stability, the use of the actual deflection of the specimen as control variable is qualitatively the same as the use of displacement. From Figs. 1 and 2 it is clear that the control by constant rates of increasing load can never lead to stable tests because load always decreases after cracking starts.

Stable fracture for SENB specimens tested in three point bending using displacement control is relatively easy to attain for materials with R-curve fracture, for which the crack resistance (i.e. G_c) increases as the crack propagates. For instance, stable fracture has been reported for materials with coarse microstructures such as silicoaluminate and high alumina refractories[3] and graphite,[11,15] for dense alumina with relatively large grain size ($d_{50} \sim 5.5\ \mu m$)[16] and for fine grained alumina–aluminium titanate composites (alumina: $d_{50} \sim 3.2$–$3.9\ \mu m$, aluminium titanate: $d_{50} \sim 2.2\ \mu m$).[16] On the contrary, for extremely brittle materials, very deep cracks and extremely stiff machines would be needed for stable fracture and thus, it is not possible in practice. In this sense, load–displacement curves showing unstable fracture or sudden load decreases ("pop-in") prior to further stable propagation (i.e. semi-stable fracture) have been reported for fine grained alumina ($d_{50} \sim 3.5\ \mu m$)[16] and silicon nitride ($d_{50} \sim 3\ \mu m$)[17].

Contrary to the above-discussed parameters, the CMOD increases through the whole fracture test, the loading of the specimen as well as during the crack growth. Thus, CMOD has been proposed and used as control parameter for stable fracture testing of high-strength concrete[14] and tetragonal zirconia stabilised with 3 mol% of Y_2O_3[18–20] specimens under conditions that would have led to unstable fracture for displacement controlled tests.

In order to perform in a routine way stable fracture tests of ceramics, a new experimental setup to perform three point bending stable fracture tests of ceramics controlled by the crack mouth opening displacement (CMOD) was developed.[21] The set up combined an electromechanical universal testing machine with a high precision optical micrometer. An electromechanical machine was chosen because the extremely small displacement variations required for the testing of brittle materials can be reached by small turns of the motor in standard electromechanical machines whereas they would require special hydraulic machines with highly precise servo valves. The use of an optical micrometer permits the measurement of the CMOD without contact with the specimen. Nowadays, the high performance of the control systems avoids the necessity of using hydraulic machines to assure rapid responses of the load frame and allows the use of control variables external to the machines such as the CMOD. Using this equipment it has been possible to test an extremely brittle ceramic such as fine grained magnesium–aluminium spinel for which a toughness value ($\sim 1\ MPa\ m^{1/2}$) about 66% lower than the previously

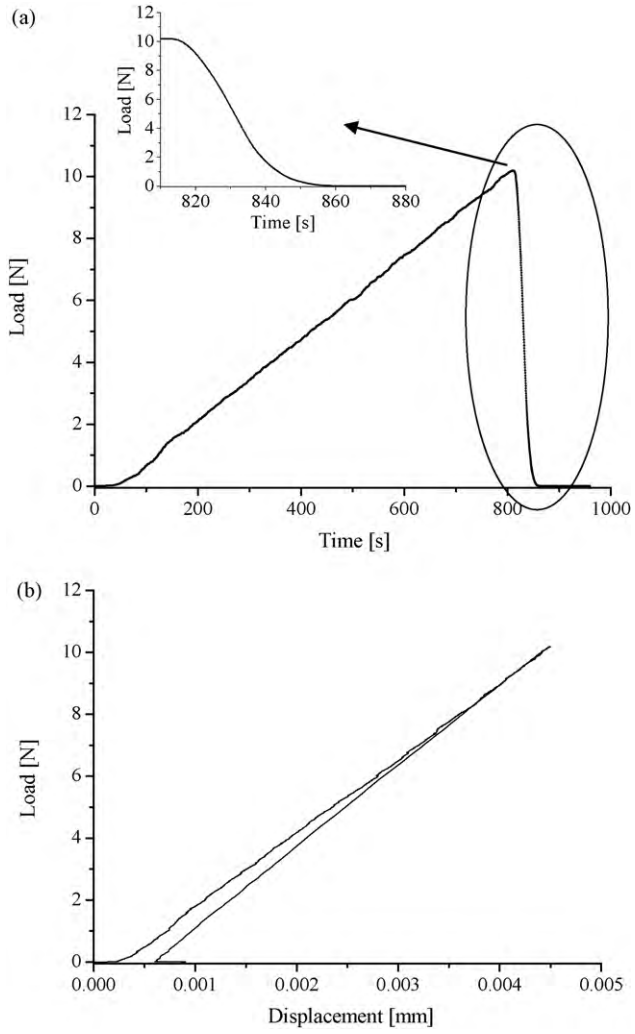

Fig. 3. Plots corresponding to a stable fracture test for a fine grained magnesium–aluminium spinel.[21] (a) Load–time plot. Monotonous load decrease with increasing times during fracture corresponding to controlled fracture is highlighted in the detail of the fracture part of the plot. (b) Load–displacement plot. During fracture the displacement has to decrease to reach stable fracture.

obtained in unstable tests (~3 MPa $m^{1/2}$)[22] was obtained. In Fig. 3 characteristic plots recorded during CMOD controlled tests for this material are shown. The shape of the load–time curve with monotonous load decreases with increasing time during fracture is characteristic of stable fracture (Fig. 3a). This behaviour is attained using a constant rate of increasing CMOD. The displacement has to decrease thorough the whole fracture process in order to maintain such rate (Fig. 3b).

In this work, after a brief description of the experimental setup, the fracture behaviour of a fine grained alumina using CMOD controlled tests is described and compared to that previously reported for displacement controlled tests for which only semi-stable fracture could be reached.[16]

2. Experimental

2.1. Material and specimen preparation

The fabrication and properties of the alumina material tested are described elsewhere.[16] Monophase alumina blocks were obtained by colloidal filtration in plaster moulds of aqueous alumina (Al_2O_3) stable suspensions. Sintering of the green blocks was performed in air in an electrical box furnace (Termiber, Spain) at heating and cooling rates of 2 °C min^{-1}, with 4 h, dwell at 1200 °C during heating and 2 h, dwell at the maximum temperature 1450 °C. The microstructural and mechanical properties for this material are summarised in Table 1.

Single Edge V-Notch Beams (SEVNB) of 4 mm thickness (B), 6 mm width (W) and 50 mm length were diamond machined from the sintered blocks. The notch was initially cut with a 300 μm wide diamond wheel (Fig. 4a). Using this pre-notch as a guide, the remaining part of the notch was done with a 150 μm wide razor blade sprinkled with 1 μm diamond paste (Fig. 4b and c). Tip radii of about 15 μm were obtained (Fig. 4c). The relative notch depth, a/W (a = notch depth, W = specimen width), was 0.5.

2.2. Mechanical testing set up

The mechanical tests were performed in a single screw, dual column and servo-controlled electromechanical universal testing machine with 50 kN load capacity and rigid frame (stiffness ~2×10^8 N/m, Microtest EM1/50, Spain). The displacement of the moving crosshead is measured and controlled by means of an optical encoder placed in the motor axis. The electronic controller (Microtest SCM3000, Spain) includes load and position channels as well as position auxiliary ones with the option to add additional strain channels for extensometers. The signal from the system for CMOD determination is directed to one of these auxiliary channels so CMOD can also be a control variable. The test specimen is placed between the rigid frame and the moving crosshead in a stainless steel three point bending test fixture with a span of 40 mm. A load cell of 5 kN was selected to assure high stiffness of the loading setup. The compliance of the machine, load cell, and supports arrangement was determined experimentally using an uncracked alumina bar (4 mm × 6 mm × 50 mm); the obtained value was 1.5×10^{-7} m/N up to 150 N.

For the CMOD measurement and control, a high precision optical micrometer Keyence LS7010 (Keyence, Japan) that

Table 1
Microstructural and mechanical parameters for the alumina material tested in this work, A-1450.[16] G_A = average grain size, ρ = relative density, E = static Young's modulus, σ_f = three point bending strength, K_{IC} = critical stress intensity factor in mode I. S.D. = standard deviation.

Material	G_A (S.D.) (μm)	ρ (S.D.) (%theoretical)	E (S.D.) (GPa)	σ_f (S.D.) (MPa)	K_{IC} (MPa $m^{1/2}$)
A-1450	3.5 (0.3)	98.1 (0.3)	379 (8)	456 (29)	2.9 2.8

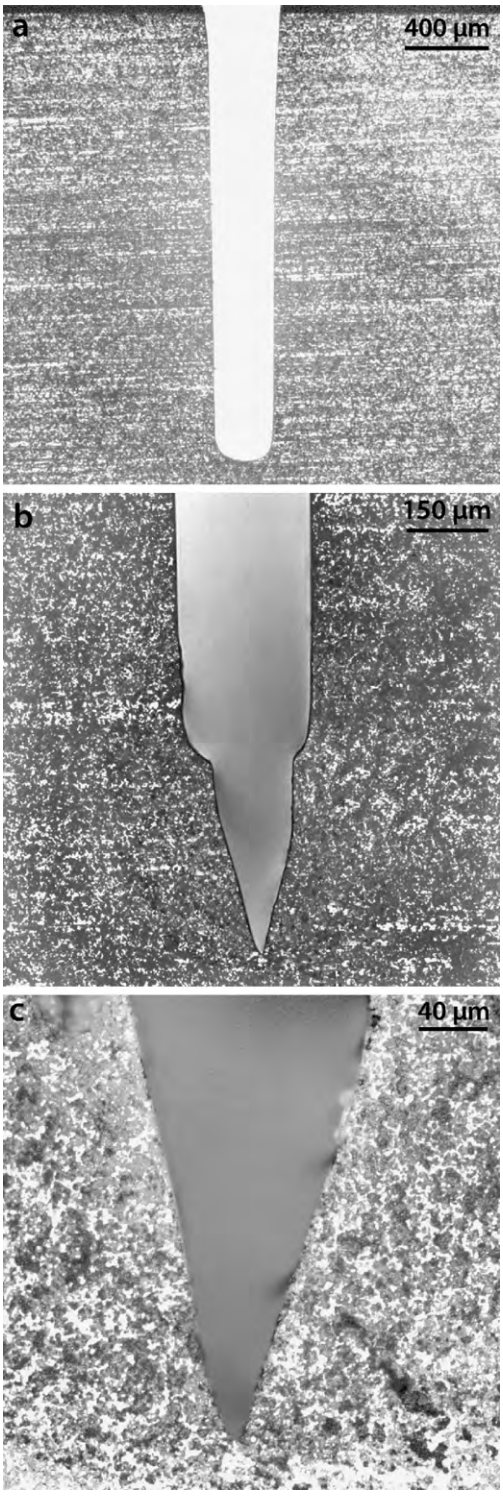

Fig. 4. Optical micrographs of a lateral surface of an alumina specimen showing the procedure to introduce the "V" notches. (a) A pre-notch is introduced with a thin (300 μm) diamond disc. (b and c) The notch tip is corrected with a razor blade with diamond past (1 μm) to reduce the tip radius below 15 μm.

incorporates a CMOS (Complementary Metal Oxide Semiconductor) camera to capture real-time image of the target was used. This optical system provides a measurement accuracy of ±0.5 μm. The equipment carries out a continuous measurement averaging up to 2400 samples/s. For the tests performed in this work, the sampling frequency of 512 s^{-1} used gave very stable readings.

The principle of measurement of the optical system is as follows. A high-intensity GaN green LED (Light-Emitting Diode) radiates light, which is changed into uniform parallel light through the special diffusion unit and collimator lens and emitted to the target in the measuring range. This parallel beam "illuminates" measurement area. Then the shadow image of the target appears on the HL-CCD (High-Speed Linear Charge Coupled Device) through the telecentric optical system. With the telecentric system of lenses the size of the image on the CCD does not change even if it moves, thus, the same accuracy all along is maintained. The output incident signal of the HL-CCD is processed by the DE (Digital Edge-detection) processor in the controller and CPU. The controller of the optical system incorporates a function of elimination of abnormal values, to improve the precision of the measurement, which detection threshold is an adjustable parameter.

The optical micrometer is attached to the lower loading support; in this way the mechanical interferences are avoided and a correct orientation of the light beam with respect to the axis of load and the bending fixture is assured. Given the small opening displacement of the notch, in order to be able to detect and measure its width during the test (the size of detectable minimum object by the system is of 0.04 mm), pins of 1.5 mm in diameter and 12 mm length are adhered to both sides of the notch assuring that they are perpendicular to the light beam. To reach the highest accuracy the tests were performed at 20 °C, with a separation between the pins of 1 mm. The repeating accuracy of the optical micrometer for this separation was checked to be ±0.06 μm using a 1.0 mm diameter round bar located in the centre of the measuring area.

The optical micrometer converts the distances detected to analog signals that are input in the controlling unit of the mechanical testing machine where the software SCM3000 (Microtest, Spain) converts them to discrete digital numbers. The whole range of the optical micrometer (6 mm) that corresponds to ±10 V of analog signal is converted in 2^{16} levels (65,536 values), thus, a theoretical resolution of 0.1 μm is obtained for the maximum range. For the tests, a smaller range of measurement of the micrometer, ±50 μm, was selected to detect the CMOD variations. In terms of analog signal, this range corresponds with a scaling value of 5 μm/V and, therefore, with a theoretical resolution of about 0.02 μm.

2.3. Testing conditions

The alumina specimens were tested in the above described experimental setup using CMOD control at rate of 1.8 μm min^{-1}. This velocity was chosen in order to use a rate of the deformation of the specimen similar to that previously used to test this material (0.005 mm min^{-1}). To determine this velocity, several specimens were tested using different CMOD rates to establish the correspondence between the displacement and CMOD rates from the time and displacement values needed to reach the maximum loads. The programmed CMOD rate was attained in all tests with variations of less than 0.02 μm min^{-1}.

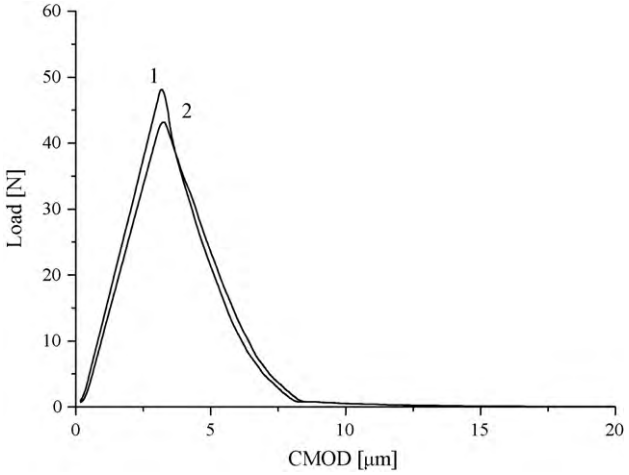

Fig. 5. Load–crack mouth opening displacement (CMOD) plots recorded during the CMOD controlled tests for two different alumina specimens showing the repeatability of the tests.

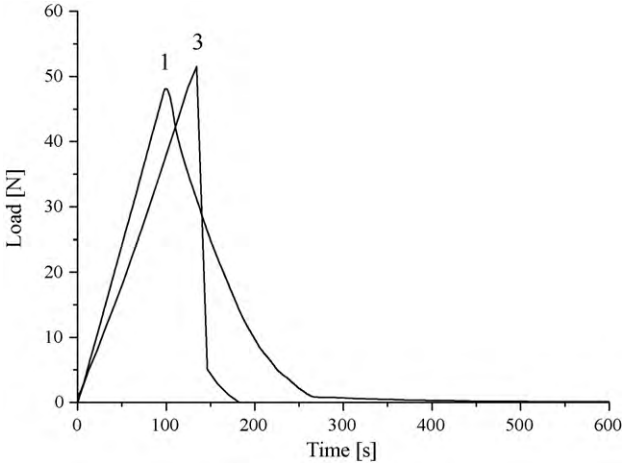

Fig. 6. Characteristic load–time plots for alumina specimens tested using different control parameters for the deformation of the specimen. (1): Crack mouth opening displacement control; stable fracture is shown. (3) Displacement control; semi-stable fracture is shown.[16]

3. Results and discussion

In which follows, the results obtained previously using the same testing and specimen geometries and displacement controlled tests[16] are compared to those obtained in this work using CMOD control. From calculations[17] using the compliance value of the whole testing system (1.5×10^{-7} m/N) and the properties of the material (Table 1), stable fracture tests could not be obtained under displacement control for any relative notch depth value for this alumina material. In fact, only semi-stable fracture was obtained for a limited number of tests of specimens with relative notch depths of 0.5 in the previously reported study. The introduction of larger notches led to the failure of the specimens during machining.

As it is shown in the load–CMOD curves of Fig. 5, similar results were obtained in this work for different specimens tested using the same CMOD rate and similar values of a/W the conditions which gave relatively low standard deviations for the fracture toughness parameters.

Fig. 6 shows characteristic load–time plots recorded using the two different control parameters. The sudden load decrease for constant time prior to further monotonous load decrease observed under displacement control is characteristic of semi-stable fracture.[16] On the contrary, in the CMOD controlled tests monotonous load decreases with increasing times as correspond to controlled fracture were always obtained. The load–displacement curves corresponding to the tests of Fig. 6 are plotted in Fig. 7. As discussed in the introduction, a decrease of displacement was needed to reach stable fracture after the maximum load which could only be attained by using CMOD control.

The critical stress intensity factor in mode I, K_{IC}, was calculated using the general expression of the stress intensity[23] and the value of the maximum load attained during the test (Eq. (1)). The onset of crack propagation was considered in the peak load.

$$K_{IC} = \frac{3SP}{2BW^{3/2}} K_\beta(\alpha) \tag{1}$$

where S is the span, P is the maximum load, B and W are the geometrical parameters defined in Section 2 and $K_\beta(\alpha)$ is a general shape function which is valid for any value of the relative notch depth ($0 \le \alpha \le 1$) and span-to-depth ratios ($\beta = S/W$) larger than 2.5 ($2.5 \le \beta \le 16$) (Eq. (2)):

$$K_\beta(\alpha) = \frac{\sqrt{\alpha}\,\{p_\infty(\alpha) + 4/\beta[p_4(\alpha) - p_\infty(\alpha)]\}}{(1-\alpha)^{3/2}(1+3\alpha)} \tag{2}$$

The $p_\infty(\alpha)$ and $p_4(\alpha)$ given by Eqs. (3) and (4) are cubic polynomial for $\beta = 4$ (equivalent to a reference beam with fixed $S/W = 4$) and $\beta = \infty$ (formally equivalent to pure bending).

$$p_\infty(\alpha) = 1.99 + 0.83\alpha - 0.31\alpha^2 + 0.14\alpha^3 \tag{3}$$

$$p_4(\alpha) = 1.9 + 0.41\alpha + 0.51\alpha^2 - 0.17\alpha^3 \tag{4}$$

The value of K_{IC} obtained for CMOD controlled tests was 2.5 ± 0.2 MPa m$^{1/2}$, about 10% lower than the value determined in semi-stable tests.[16]

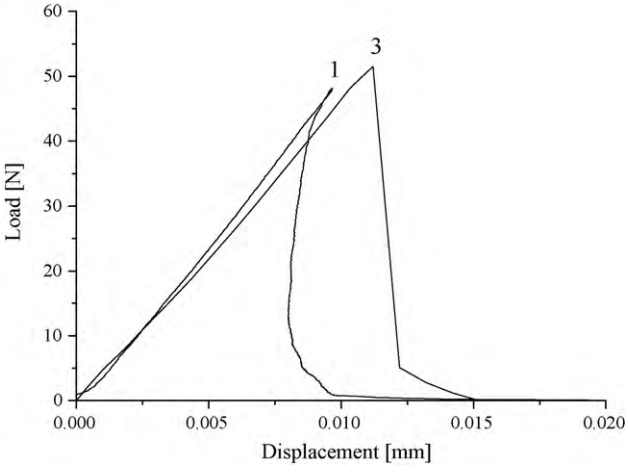

Fig. 7. Load–displacement plots corresponding to the test of Fig. 6. (1) Crack mouth opening displacement control; a decrease of displacement after the maximum load is needed to reach stable fracture tests. (3) Displacement control.[16]

From K_{IC} and Young's modulus (Table 1), the critical energy release rate, G_{IC}, was calculated according to the analysis of Irwin for plane strain conditions (Eq. (5)):

$$G_{IC} = \frac{K_{IC}^2}{E'} \tag{5}$$

where $E' = E/(1-\nu^2)$ is the generalized Young's modulus for plane strain (E is the Young's modulus and ν is the Poisson's ratio). The Poisson's ratio for dense and fine grained alumina is 0.223 ± 0.004.[24] The value of G_{IC} obtained was $16.4 \pm 2.3\,J\,m^{-2}$ that is about 20% lower than the value previously obtained in semi-stable tests.[16]

The work of fracture, γ_{WOF}, was calculated by dividing the work done on the specimen to propagate the crack, calculated as the integral of the load–displacement plot, by the area of the newly created surfaces (Eq. (6)). For parallelepiped bars with straight trough notches tested in flexure, this area is twice the area of the unnotched part of the cross-section of the specimens.

$$\gamma_{WOF} = \frac{A}{2B(W-a)} \tag{6}$$

where A is the area under the load–displacement curves and B, W and a were defined in Section 2.

The value of γ_{WOF} obtained was $7.0 \pm 0.3\,J\,m^{-2}$ that is about 30% lower than the value obtained in semi-stable tests.[16]

4. Conclusions

An experimental setup to perform stable fracture tests in an electromechanical machine using the analog output from an optical micrometer was developed. This set up allows using the crack mouth opening displacement (CMOD) as a control parameter for fracture toughness testing.

Stable fracture tests can be performed for brittle ceramics by using the CMOD as control parameter and three points bending of Single Edge V-Notch Beams as testing geometry.

Stable fracture tests for fine grained alumina performed using this device have given fracture toughness parameters ($K_{IC} = 2.5 \pm 0.2\,MPa\,m^{1/2}$, $G_{IC} = 16.4 \pm 2.3\,J\,m^{-2}$, $\gamma_{WOF} = 7.0 \pm 0.3\,J\,m^{-2}$) lower than those determined in semi-stable tests: about 10%, 20% and 30% for critical stress intensity factor in mode I, critical energy release rate and work of fracture, respectively.

Acknowledgements

This work has been supported by MCI-MAT2009-14448-C02 and PET2008-0113 and Microtest S.A. (Spain). Discussions with Prof. J.Y. Pastor from ETSI Caminos, Canales y Puertos (Madrid) are gratefully acknowledged.

References

1. Ghosh A, Jenkins MG, White KW, Kobayashi AS, Bradt RC. Elevated-temperature fracture resistance of a sintered α-silicon carbide. *J Am Ceram Soc* 1989;**72**(2):242–7.
2. Nakayama J. Direct measurement of fracture energies of brittle heterogeneous materials. *J Am Ceram Soc* 1965;**48**(11):583–7.
3. Nakayama J, Abe H, Bradt RC. Crack stability in the work-of-fracture test: refractory applications. *J Am Ceram Soc* 1981;**64**(11):671–5.
4. Tattersall HG, Tappin G. The work of fracture and its measurement in metals, ceramics and other materials. *J Mater Sci* 1966;**1**:296–301.
5. Calomino AM, Brewer DN. Controlled crack growth specimen for brittle systems. *J Am Ceram Soc* 1992;**75**(1):206–8.
6. Sørensen BF, Horsewell A, Jørgensen O, Kumar AN, Engbæk P. Fracture resistance measurement method for in situ observation of crack mechanisms. *J Am Ceram Soc* 1998;**81**(3):661–9.
7. Wan D, Bao Y, Peng J, Zhou Y. Fracture toughness determination of $Ti_3Si(Al)C_2$ and Al_2O_3 using a single gradient notched beam (SGNB) method. *J Eur Ceram Soc* 2009;**29**:763–71.
8. Kuszyk JA, Bradt RC. Influence of grain size on effects of thermal expansion anisotropy in $MgTi_2O_5$. *J Am Ceram Soc* 1973;**56**(8):420–3.
9. Sørensen BF, Brethe P, Skov-Hansen P. Controlled crack growth in ceramics: the DCB specimen loaded with pure moments. *J Eur Ceram Soc* 1996;**16**(9):1021–5.
10. Ebrahimi ME, Chevalier J, Fantozzi G. *R*-curve evaluation and bridging stress determination in alumina by compliance analysis. *J Eur Ceram Soc* 2003;**23**(6):943–9.
11. Sakai M, Urashima K, Inagaki M. Energy principle of elastic–plastic fracture and its application to the fracture mechanics of a polycrystalline graphite. *J Am Ceram Soc* 1983;**66**(12):868–74.
12. Baratta FI, William AD. Crack stability in simply supported four-point and three-point loaded beams of brittle materials. *Mech Mater* 1990;**10**:149–59.
13. Sigl LS. On the stability of cracks in flexure specimens. *Int J Fract* 1991;**51**:241–54.
14. Biolzi L, Cangiano S, Tognon G, Carpinteri A. Snap-back softening instability in high-strength concrete beams. *Mater Struct* 1989;**22**:429–36.
15. Davidge RW, Tappin G. The effective surface energy of brittle materials. *J Mater Sci* 1968;**3**:165–73.
16. Bueno S, Berger MH, Moreno R, Baudín C. Fracture behaviour of microcrack free alumina–aluminium titanate ceramics with second phase nanoparticles at alumina grain boundaries. *J Eur Ceram Soc* 2008;**28**:1961–71.
17. Bar-On I, Baratta FI, Cho K. Crack stability and its effect on fracture toughness of hot-pressed silicon nitride beam specimens. *J Am Ceram Soc* 1996;**79**(9):2300–8.
18. Pastor JY, Planas J, Elices M. Ambient and high-temperature stable fracture tests in ceramics: applications to yttria-partially-stabilized zirconia. *J Am Ceram Soc* 1993;**76**(11):2927–9.
19. Pastor JY, Planas J, Elices M. A new technique for fracture characterization of ceramics at room and at high temperature. *J Test Eval* 1995;**23**(3):209–16.
20. Pastor JY, Planas J, Elices M. Ensayos de fractura estables en materiales cerámicos. *Bol Soc Esp Ceram V* 1992;**31**(4):322–5.
21. Baudín C, García A, Hernández J, López M. Anales de Mecánica de la Fractura. In: Proceedings of the Conferencia Ibérica de Fractura e Integridad Estructural 2010, vol. 1. Controlled fracture tests of brittle ceramics, Secretaría del Grupo Español de Fractura, Madrid, Spain; 2010. p. 291–5.
22. Baudín C, Martínez R, Pena P. High-temperature mechanical behavior of stoichiometric magnesium spinel. *J Am Ceram Soc* 1995;**78**(7):1857–62.
23. Guinea GV, Pastor JY, Planas J, Elices M. Stress intensity factor, compliance and CMOD for a general three-point-bend beam. *Int J Fract* 1998;**89**:103–16.
24. Burgos-Montes O, Moreno R, Baudín C. Effect of mullite additions on the fracture mode of alumina. *J Eur Ceram Soc* 2010;**30**:857–63.